The Astrophysical Journal, 671:1079–1083, 2007 December 20


# THE KINETIC SUNYAEV-ZEL'DOVICH EFFECT DUE TO THE ELECTRONS OF OUR GALAXY

Amir Hajian,[1,2] Carlos Hernández-Monteagudo,[3] Raul Jimenez,[3] David Spergel,[2] and Licia Verde[3]

*Received 2007 June 14; accepted 2007 August 7*


## ABSTRACT

We compute the effect of local electrons on the CMB temperature anisotropies. The number density and distribution of free electrons in our Galaxy has been accurately measured from pulsar dispersion measurements. Because of their distribution, the dynamics of our Galaxy, and the Galaxy peculiar velocity with respect to the Hubble flow, these free electrons leave a frequency-independent imprint on the cosmic microwave background (CMB). In particular, the coherent motion of the free electrons with respect to us and to the CMB rest frame produce a kinetic Sunyaev-Zel'dovich signal. We compute this effect and we note that the large-scale antisymmetry of the signal gives it an angular power spectrum with a sawtooth pattern, where even multipoles are suppressed with respect to the odd ones. We find the signal to be small ($\sim 2\ \mu$K) and subdominant compared to the primary CMB and other foreground signals. However, since the parameters of this model are constrained by other independent astrophysical observations, it can be taken into account if more precise measurements of the primordial signal are required.


*Subject headings:* cosmic microwave background — Galaxy: kinematics and dynamics

*Online material:* color figures

## 1. INTRODUCTION AND BACKGROUND

The motion of the ionized gas in our Galaxy leaves its imprint on the CMB through the kinetic Sunyaev-Zel'dovich Effect (Sunyaev & Zel'dovich 1980; Hogan 1992). These distortions are spectrally indistinguishable from the CMB. Thompson scattering of CMB photons from a line element $ds$ of free electrons with optical depth $d\tau$ along the line of sight determined by the unit vector $\hat{\boldsymbol{n}}$ gives a correction to the CMB temperature:

$$dT(\hat{\boldsymbol{n}}) = -d\tau\, \delta T_{\rm CMB}(\hat{\boldsymbol{n}}) - d\tau\, \frac{\boldsymbol{v}}{c} \cdot \hat{\boldsymbol{n}} T_{\rm CMB}(\hat{\boldsymbol{n}}). \quad (1)$$

Thus, there are two terms, the first is a blurring of the CMB anisotropies [$\delta T_{\rm CMB}(\hat{\boldsymbol{n}}) = T_{\rm CMB}(\hat{\boldsymbol{n}}) - T_0$, where $T_0 = \langle T_{\rm CMB} \rangle$], while the second is a generation of new anisotropies: the kinetic SZ (kSZ) effect.

If $\delta T_{\rm CMB} \ll T_0$ (i.e., we are in a coordinate system where the CMB has zero dipole[4]) and $v/c > 10^{-5}$, the second term dominates. Thus, the integrated effect along the line of sight, for $\tau \ll 1$ is given by

$$\frac{\delta T}{T} = -\int n_e \sigma_{\rm T} \frac{v_r}{c}\, dl \sim \tau(\hat{\boldsymbol{n}}) \frac{v_r(\hat{\boldsymbol{n}})}{c}, \quad (2)$$

where $v_r \equiv \boldsymbol{v} \cdot \hat{\boldsymbol{n}}$, $n_e$ denotes the electron density, and $\sigma_{\rm T}$ the Thompson cross section. Given that plausible velocities are of the orders of few $\times 100$ km s$^{-1}$ (the largest velocity, 620 km s$^{-1}$, is that of the infall of the local group to the Great Attractor) only $\tau > 10^{-3}$ yields a measurable signal. Such high optical depth implies a number density of electrons and baryonic mass that is only consistent with that present in the disk of our own Galaxy.

In this case, the velocity can be written as a sum of the Sun's velocity as measured from the CMB dipole, $v_{\rm dipole}$, and the gas velocity with respect to the Sun. Note that in a coordinate system where the Sun is at rest, the contribution for $v_{\rm dipole}$ is interpreted as a blurring of anisotropies (first term in the LHS of eq. [1]), the anisotropies being the CMB dipole.

Here, we compute the kSZ signature of the Galaxy on the CMB sky. While this signal is subdominant compared to other foreground signals and small compared to the intrinsic CMB anisotropy, it is a component that must be there and that can be modeled as we illustrate below. We assume a simple model for the velocities of the free electrons in our Galaxy that includes an axisymmetric model for the rotation around the Galactic center with the same speed as the luminous matter, $\boldsymbol{v}_{\rm rot}$, and a bulk motion, $\boldsymbol{v}_{\rm bulk}$ of the Galactic center with respect to the Hubble flow. We neglect the higher order corrections to these assumptions such as blurring of intrinsic CMB anisotropies (first term in eq. [1]). The total velocity of the free electrons with respect to the CMB rest frame is the vector sum of the above velocities, $\boldsymbol{v} = \boldsymbol{v}_{\rm rot} + \boldsymbol{v}_{\rm bulk}$. The bulk velocity, $\boldsymbol{v}_{\rm bulk}$, can be derived from the observed dipole of the CMB as $\boldsymbol{v}_{\rm bulk} = \boldsymbol{v}_{\rm dipole} - \boldsymbol{v}_{\odot}$, where $\boldsymbol{v}_{\odot}$ is the linear velocity of the rotation of the Sun around the Galactic center. Therefore, we have $\boldsymbol{v} = \boldsymbol{v}_{\rm dipole} + (\boldsymbol{v}_{\rm rot} - \boldsymbol{v}_{\odot})$. The radial part of this velocity is the $v_r$ that appears in equation (2) and is given by

$$v_r = v_{\rm los} + \boldsymbol{v}_{\rm dipole} \cdot \hat{\boldsymbol{n}}, \quad (3)$$

where $v_{\rm los} = (\boldsymbol{v}_{\rm rot} - \boldsymbol{v}_{\odot}) \cdot \hat{\boldsymbol{n}}$ is the line-of-sight velocity with respect to the Sun.

## 2. THE MODEL FOR THE GALACTIC DISTRIBUTION OF FREE ELECTRONS

We use the Cordes and Lazio (Cordes & Lazio 2002) model (hereafter NE2001) for the distribution of free electrons in our Galaxy. Cordes & Lazio (2002) combine the measurements of the dispersion measures (DM) of pulsars, temporal broadening of pulses from pulsars with large DM, scintillation bandwidth measurements of low-DM pulsars, angular broadening of Galactic and extra-Galactic sources and emission measures to infer the

[1] Department of Physics, Jadwin Hall, Princeton University, Princeton, NJ 08542; ahajian@princeton.edu.

[2] Department of Astrophysical Sciences, Peyton Hall, Princeton University, Princeton, NJ 08544; dns@astro.princeton.edu.

[3] Department of Physics and Astronomy, University of Pennsylvania, 209 South 33rd Street, Philadelphia, PA 19104; carloshm@astro.upenn.edu, raulj@physics.upenn.edu, lverde@physics.upenn.edu.

[4] Note that this will not be the case in a coordinate system where the CMB has a large dipole, for example in a coordinate system where the Sun is at rest.

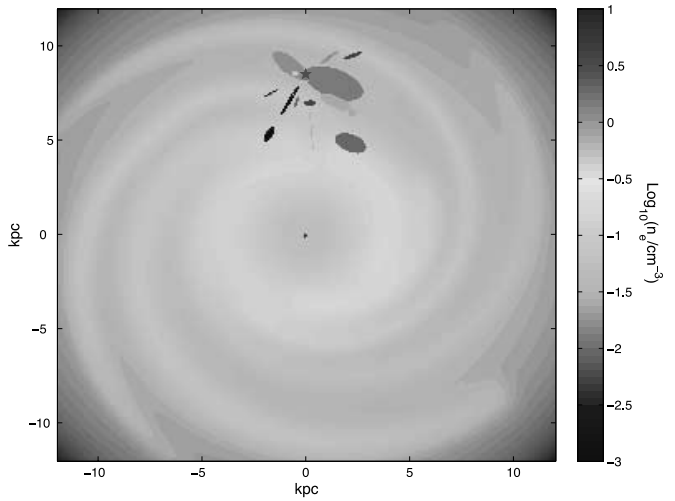


FIG. 1.—Distribution of the free electrons in our Galaxy, log ($n_e$), based on NE2001. The $n_e$ is shown at the Galactic plane, $z = 0$, and is maximum at the Galactic center. The position of the Sun is denoted by a star and the small overdense region close to the Sun is the Gum Nebula. [*See the electronic edition of the Journal for a color version of this figure.*]

distribution of the free electrons in the Galaxy responsible for pulsar dispersion measures and a spatial model of the warm ionized component of the interstellar gas.

The electron density distribution is given by the sum of two axisymmetric components (the thick disk and the thin disk) and a spiral arm component, combined with terms that describe specific regions in the Galaxy. The local interstellar medium is modeled with multiple components: (1) four low-density regions near the Sun: a local hot bubble centered on the Sun's location, the North Polar Spur, a local superbubble, and another low-density region, (2) the Galactic center component, (3) the Gum Nebula and the Vela supernova remnant, (4) regions of intense scattering (clumps), and (5) regions of low density (voids).

Figure 1 shows the Galactic distribution of the free electrons, $n_e$, at the Galactic plane, based on the NE2001 model. The position of the Sun is denoted by a star. The high electron density spot on the left side of the Sun is the Gum Nebula.

## 3. KINEMATICS OF THE DIFFERENTIAL ROTATION OF THE GALAXY

We consider an axisymmetric model for the rotation of the Milky Way. The orbits in this model are circular and the angular velocity at point $\boldsymbol{R}$ is $\Omega(R)$, where $R = |\boldsymbol{R}|$. We are interested in the line-of-sight velocity, $v_{\rm los}$, the projection of the velocity of each particle relative to the Sun along the vector connecting the Sun to that point, $(\boldsymbol{R} - \boldsymbol{R}_\odot)$. Here, $\boldsymbol{R}_\odot$ denotes the position of the Sun in the Galactocenteric coordinates. Therefore,

$$v_{\rm los} = \hat{\boldsymbol{R}}_{\rm los} \cdot (\boldsymbol{v}_{\rm rot} - \boldsymbol{v}_\odot), \tag{4}$$

where $\hat{\boldsymbol{R}}_{\rm los} = (\boldsymbol{R} - \boldsymbol{R}_\odot)/|\boldsymbol{R} - \boldsymbol{R}_\odot|$. Following the standard discussion in Binney & Merrifield (1998) the line-of-sight velocity $v_{\rm los}$ can be expressed as a function of longitude, $l$, on the celestial sphere and $R$:

$$v_{\rm los}(l, R) = [\Omega(R) - \Omega(R_\odot)]R_\odot \sin l. \tag{5}$$

The disk of the Milky Way consists of three parts: the central disk at $R < 3$ kpc, the inner disk, $R_0 > R > 3$ kpc, and the outer disk, $R > R_0$. The determination of the $v_{\rm los}$ is different in each of the three parts.

For the inner disk, the observable is the terminal velocity, $v^t_{\rm los}(l_1)$, along each line of sight, $l_1$. The terminal velocity is defined as follows: consider the smallest ring—centered on the Galactic center—that intercepts the line of sight. The line of sight is thus tangent to this ring, and the radius of the ring is $R = R_\odot \sin l_1$. The terminal velocity is the line-of-sight velocity of the ring at the tangent point. The 21 cm line and CO emission-line observations are used to estimate $v_{\rm los}$ (e.g., Rougoor & Oort 1960), and the distance to the tangent point is determined by geometry. The circular velocity of the ring can be calculated using $v^t_{\rm los}(l)$ values reported in chapter 9 of Binney & Merrifield (1998) and equation (5),

$$\begin{aligned} v_c(R) &= v^t_{\rm los}(l_1) + v_c(R_0) \sin l_1, \\ \sin l_1 &= R/R_0, \end{aligned} \tag{6}$$

and therefore

$$v_{\rm los}(l, R) = [v_c(R)(R_0/R) - v_c(R_0)] \sin l. \tag{7}$$

In the outer disk, distances are not so easily determined and thus distances and velocities are obtained either by observations of Cepheid variables or by main-sequence fitting of a young cluster and radio-line observations of associated molecular gas (see Brand & Blitz 1993, and references therein).

The measurement of $v_{\rm los}$ is then given by

$$v_{\rm los}(l, R) = W(R) \sin l, \tag{8}$$

where $W(R) \equiv R_0[\Omega(R) - \Omega(R_0)]$ is given as a function of $R/R_0$ in Brand & Blitz (1993). Note however that the errors associated to the distance $R$ and the errors assigned to a given measurement of $W(R)$ increase dramatically for $R > 1.5R_0$, and therefore very little can be said about $v_{\rm los}$ for radii larger than $2R_0$ (Binney & Dehnen 1997).

The velocities in the central disk are more complicated. Here, we calculate them in the same way as the inner disk velocities: we extrapolate the terminal velocities of the central disk from those of the inner disk. This approximation however does not significantly affect our final result because the $v_{\rm los}$ is small close to the Galactic center where $n_e$ is large. In addition, the effect of noncircular motions such as axisymmetric expansion, oval distortions of the orbits, and random motions act as a correction to the above model. For simplicity we ignore these corrections and only consider circular motions; as discussed in chapter 9 of Binney & Merrifield (1998) this simplified model works well outside of the central (3 kpc) disk.

## 4. THE KINETIC SZ PATTERN

We now separately compute the contribution to the kSZ signal due to the rotation of the Galaxy (§ 4.1) and the contribution due to the motion of the Galaxy with respect to the CMB rest frame (§ 4.2). We use the free-electron density model of NE2001 and the above model for the velocity field of the Galaxy to obtain the Galaxy kSZ pattern. As the velocity field, $v_{\rm los}$, is defined with respect to the Sun, there will be an additional contribution due to $\boldsymbol{v}_{\rm dipole}$.

### 4.1. *Motion within the Galaxy*

We assume the Sun is located at $(x, y, z) = (0.0, 8.5, 0.0)$ kpc in Galactocenteric coordinates, $R_0 = 8.5$ kpc, and $v_\odot = 220\ {\rm km\ s^{-1}}$.

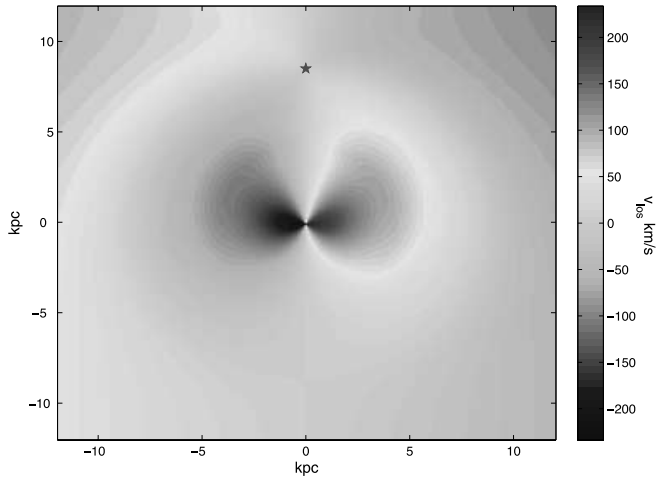


FIG. 2.—Line-of-sight velocity relative to the Sun, $v_{los}$, on the plane of the Galaxy. The position of the Sun is denoted by a star; $v_{los}$ is negative when a point moves toward the Sun. [*See the electronic edition of the Journal for a color version of this figure.*]

The kSZ effect is calculated using equation (2). We integrate equation (2) along the line of sight:

$$\Delta T(\hat{n}) = -\frac{\sigma_T}{c} T_0 \sum_{i=1}^{N} n_e(r_i\hat{n}) v_{los}(r_i\hat{n}) \Delta r$$

$$\simeq -(4.1\ \mu\mathrm{K}) \sum_{i=1}^{N} \left[\frac{n_e(r_i\hat{n})}{1\ \mathrm{cm}^{-3}}\right] \left[\frac{v_{los}(r_i\hat{n})}{220\ \mathrm{km\ s}^{-1}}\right] \left(\frac{\Delta r}{\mathrm{kpc}}\right), \quad (9)$$

where $r_i = r_{i-1} + \Delta r$ with $r_0 = 0$. While the velocities in the outer disk are not known beyond $r \sim 1.5$–$2\ R_0$, most of the contribution comes from the central and inner disks, hosting the largest electron densities and peculiar velocities. Thus, we only consider electrons that are within the $r = 2R_0$ sphere. The result is shown in Figure 3, below.

The kSZ pattern is antisymmetric; its main features are a cold and a hot spot at the two sides of the Galactic center with $|l| < 90^\circ$ and $\delta T_{max} \sim 2\ \mu$K. These spots come from the regions in the inner disk with the highest $v_{los}$ (see Fig. 2). There are weaker warm and cold spots at larger longitudes, $|l| > 90^\circ$, caused by the rotating electrons in the outer disk. The kSZ signal is zero at $l = 0^\circ$ and $180^\circ$, where $v_{los} = 0$. Both the Galactic center and the Gum Nebula, which have the larger $n_e$, happen to fall in regions with very small $v_{los}$ and therefore do not contribute much to the kSZ due to the rotation of the Galaxy.

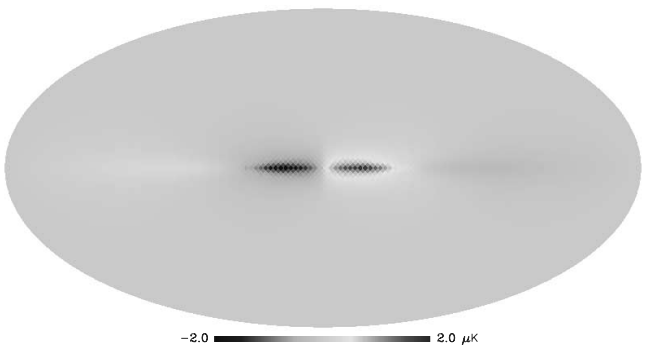


FIG. 3.—Map of the predicted kinetic SZ signal caused by the rotation of the free electrons in the disk of our Galaxy. [*See the electronic edition of the Journal for a color version of this figure.*]

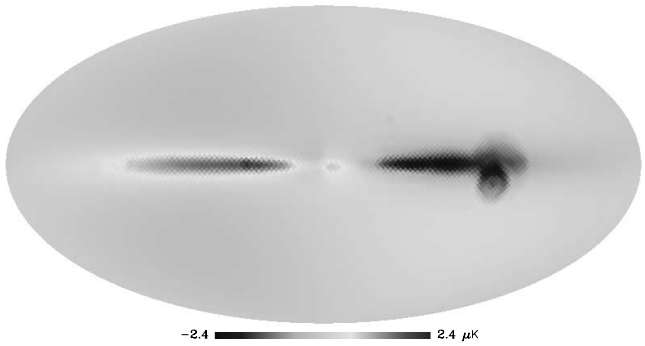


FIG. 4.—Dipole subtracted map of the effect of the free electrons in our Galaxy due to the rotation and the bulk motion of the Milky Way. [*See the electronic edition of the Journal for a color version of this figure.*]

### 4.2. *Motion of the Galaxy*

The second term of equation (3) arises from the bulk motion of the Galaxy with respect to the CMB rest frame. We consider the dipole velocity to be $v_{dipole} = 371$ km s$^{-1}$ in the direction of $(l, b) = (264^\circ, 48^\circ)$.

This bulk motion generates a kSZ signal bigger than the one due to the rotation of the Galaxy. The signal can be interpreted as a suppression of the dipole due to the free electrons in the Galaxy; thus, it is a negative dipole modulated by the line-of-sight integration of the electron distribution $n_e$. The signal of the Galactic Center and the Gum Nebula feature prominently because of their high density.

### 4.3. *The Combined Effect*

We add this to the map of Figure 3 to obtain the total kSZ signal generated by the free electron distribution in our Galaxy. The resulting map *after dipole subtraction* is shown in Figure 4. This pattern is still antisymmetric and mostly lies in the plane of the Galaxy but it overrides the fourfold pattern of Figure 3. The cold spot centered at $(l, b) = (-90^\circ, 0^\circ)$ is due to the overdensity of the free electrons in the Gum Nebula, and the warm

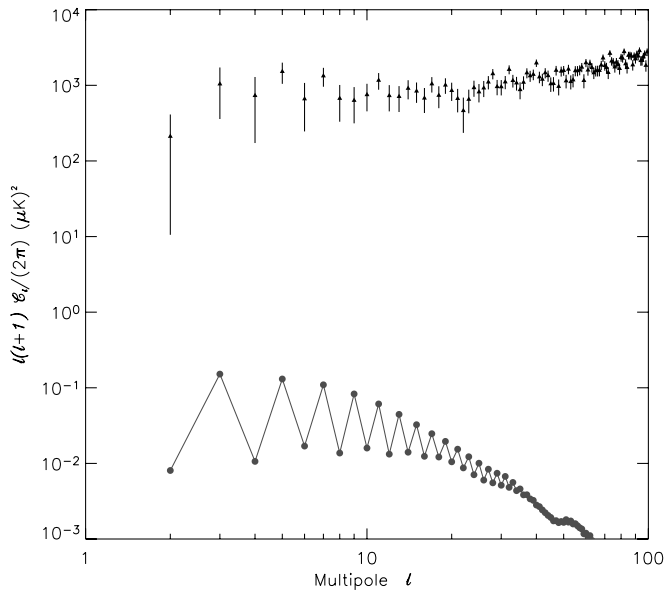


FIG. 5.—Angular power spectrum $C_l$ for the predicted kinetic SZ signal (*filled circles*). Measurements from *WMAP* (3 yr data) are displayed as triangles. [*See the electronic edition of the Journal for a color version of this figure.*]

spot at the center of the Galaxy reflects the high $n_e$ there. Figure 5 shows the angular power spectrum of the kSZ signal. Most of the power resides at large scales (low $l$-values), but its contribution to the intrinsic CMB power spectrum remains around the 0.01% level.

An interesting feature of the above pattern is the sawtooth shape of its angular power spectrum. This is due to the large-scale antisymmetry of the kSZ pattern, which suppresses the even multipoles with respect to the odd ones. The pattern quickly disappears at higher multipoles.

## 5. DISCUSSION AND CONCLUSION

We have computed the kinetic SZ contribution to the CMB anisotropies due to the coherent motion of the free electrons in the disk of our Galaxy. We used the model of Cordes & Lazio (2002) for the Galactic distribution of free electron and kinematics of the differential rotation of our Galaxy to compute the line-of-sight velocity with respect to the Sun. The bulk motion of our Galaxy causes another effect that is comparable to this effect. We calculate the anisotropic pattern due to the combination of these effects and show the result in Figure 4.

This kSZ signal is subdominant compared to the primary CMB and other foregrounds, but since the parameters of this model are constrained by other independent astrophysical observations, this contribution to the anisotropy can be easily modeled and subtracted out. There are three major sources of uncertainties in our calculations. (1) uncertainties in the circular velocity model are typically of 10% (Binney & Merrifield 1998), which should propagate linearly into the temperature map. A comparison with a simplified model for the circular velocity which assumes a flat rotation curve for the Galaxy, yields differences of the order of 5%. As discussed in Binney & Merrifield (1998), neglecting the effect of the noncircular motion is a good approximation outside of the central disk (3 kpc). (2) Uncertainties in the electron distribution; we are adopting NE2001 model which characterizes the density of free electrons in the Galaxy as a function of a set of parameters. The best-fit values for these parameters are provided by Cordes & Lazio (2002). In order to quantify the impact of the uncertainties of these parameters, we remove the Galactic arms from the model and recomputed the kSZ map. We find changes at the level of 10% on average and 30% at the tangent points. (3) The position of the Sun is another uncertain parameter. In our calculations we have chosen the Sun to be at $(0, 8.5, 0)$ kpc. To quantify the effect of varying this parameter, we move the Sun to $(0, 7.5, 0)$ kpc (closer to the center of the Galaxy), finding differences of the order of 3%.

This effect has been independently studied by another group (Waelkens et al. 2007), and our results agree. The polarization signal of the Thompson scattering from the free electrons in the local universe was studied in Hirata et al. (2005).

In Figure 6 we show *WMAP*'s ILC map, which Hinshaw et al. (2007) smoothed with a $420'$ beam, and a map in Galactic coordinates of the integral of the line-of-sight velocity due to the rotation of the Galaxy. Note the similarity between the maps. However, a posteriori statistics based on this similarity are misleading, as we do not know any physical mechanism that can relate the above velocity map to the large-scale fluctuations in ILC map. We find another similarity in the sawtooth pattern of the angular power spectrum of the kSZ map (Fig. 5). This pattern has the same shape as the full-sky power spectrum derived from *WMAP*'s ILC map; at low-$l$, even multipoles are suppressed with respect to the odd ones. Although the kSZ signal is too small to explain the suppression of the even multipoles in the *WMAP* data, it suggests that a mechanism that boosts the above kSZ signal by about 2 orders of magnitude might explain the sawtooth pattern of the ILC power spectrum and other peculiarities of the two-point correlation of the ILC map (such as the anticorrelation at $\theta = 180^\circ$; Hajian 2007). Any element in our Galaxy that does not emit but only scatters CMB photons would be a good candidate for the above process, since it would preserve the thermal CMB spectrum and enhance the kSZ signal. We do not know any physical mechanism with the above properties. The intriguing similarity in Figure 6 is, therefore, more likely a warning about the dangers of a posteriori analysis than the signature of novel physics.

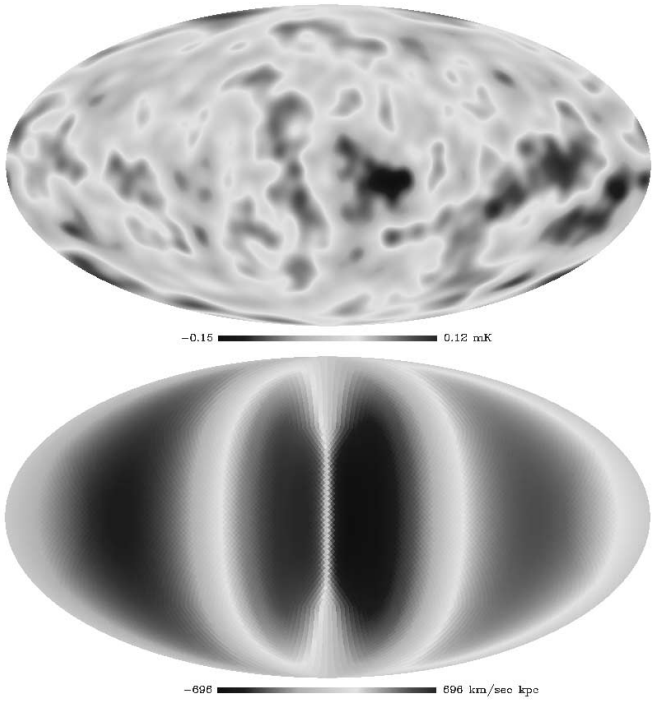


FIG. 6.— *Top*: ILC map based on the *WMAP* 3 yr data, smoothed with a $420'$ beam. *Bottom*: Map of the integral of the line-of-sight velocity relative to the Sun in Galactic coordinates. Both maps happen to have a similar structure on the large scales. [*See the electronic edition of the Journal for a color version of this figure.*]

A. H. thanks Joseph Taylor and Andre Waelkens for enlightening discussions and Eric Auborg for his comments on the manuscript. Some of the results in this paper have been derived using the HEALPix package (Gorski et al. 2005). We acknowledge the use of the Legacy Archive for Microwave Background Data Analysis (LAMBDA). Support for LAMBDA is provided by the NASA Office of Space Science. A. H. acknowledges support from NASA grant LTSA03-0000-0090. L. V. and C. H. M. are supported in part by NASA grant ADP03-0000-009 and ADP04-0000-093. R. J., L. V., C. H. M., and D. N. S. are supported in part by NSF PIRE-0507768 grant. L. V., R. J., and C. H. M. thank the physics department of Princeton University for hospitality while part of this work was being carried out.

REFERENCES

Binney, J., & Dehnen, W. 1997, MNRAS, 287, L5
Binney, J., & Merrifield, M. 1998, Galactic Astronomy (Princeton, Princeton Univ. Press)
Brand, J., & Blitz, L. 1993, A&A, 275, 67
Cordes, J. M., & Lazio, T. J. W. 2002, preprint (astro-ph/0207156)
Gorski, K. M., Hivon, E., Banday, A. J., Wandelt, B. D., Hansen, F. K., Reinecke, M., & Bartelman, M. 2005, ApJ, 622, 759
Hajian, A. 2007, preprint (astro-ph/0702723)
Hinshaw, G., et al. 2007, ApJS, 170, 288
Hirata, C. M., Loeb, A., & Afshordi, N. 2005, Phys. Rev. D, 71, 063531
Hogan, C. J. 1992, ApJ, 398, L77
Rougoor, G. W., & Oort, J. H. 1960, Proc. Nat. Acad. Sci., 46, 1
Sunyaev, R. A., & Zel'dovich, I. B. 1980, MNRAS, 190, 413
Waelkens, A., Maturi, M., & Ensslin, T. 2007, preprint (arXiv:0707.2601)